

# Ba(Zn<sub>1/3</sub>Ta<sub>2/3</sub>)O<sub>3</sub> perovskite ceramics doped with Nb<sup>5+</sup>, Ce<sup>4+</sup> or Yb<sup>3+</sup>

C. BUSUIOC<sup>a,b</sup>, S.I. JINGA<sup>a\*</sup>, S. STOLERIU<sup>a</sup>, L. NEDELICU<sup>b</sup>, E. ANDRONESCU<sup>a</sup>

<sup>a</sup>University "Politehnica" of Bucharest, RO-011061, Bucharest, Romania

<sup>b</sup>National Institute of Materials Physics, RO-077125, Magurele - Bucharest, Romania

Ba(Zn<sub>1/3</sub>Ta<sub>2/3</sub>)O<sub>3</sub> (BZT) perovskite material has stimulated a large interest due to its excellent dielectric properties in microwave frequency range, enabling the miniaturization of communications devices. In this work, BZT ceramics were prepared by the conventional solid-state reaction method, being doped with Nb<sup>5+</sup>, Ce<sup>4+</sup> or Yb<sup>3+</sup>. BZT resonators were compositional, structural, morphological and electrical characterized. The influence of the dopants and sintering temperature on the microwave dielectric properties of BZT samples was investigated. The resonator doped with 0.5 mol% Nb<sub>2</sub>O<sub>5</sub> and sintered at 1600 °C / 2 h exhibits the best dielectric behaviour:  $\epsilon_r \sim 25.9$  and  $Q \times f \sim 159$  THz.

(Received February 10, 2012; accepted April 11, 2012)

**Keywords:** Perovskite, Dielectric, Resonator, Microwave

## 1. Introduction

Complex perovskite materials with a high permittivity ( $\epsilon_r$ ), a high quality factor ( $Q$ ) and a low temperature coefficient of the resonant frequency ( $\tau_f$ ) are used as dielectric resonators in mobile communications devices, which demand the miniaturization of the size and weight, as well as temperature stability. [1, 2].

Ba(Zn<sub>1/3</sub>Ta<sub>2/3</sub>)O<sub>3</sub> (BZT) compound belongs to  $A(B'_{1/3}B''_{2/3})O_3$  ( $A = \text{Ba, Sr, Ca}$ ;  $B' = \text{Mg, Zn, Ni, Co, Sr, Ca, Mn, Cd}$ ;  $B'' = \text{Nb, Ta}$ ) complex perovskite family, that is the most widely studied class of microwave ceramic materials; the substitution of different cations in  $A$ ,  $B'$  or  $B''$  sites allows the tailoring of the dielectric properties [1, 3]. BZT exhibits a moderate dielectric constant ( $\epsilon_r \sim 28$ ), a high quality factor ( $Q \times f \sim 168$  THz) and a low temperature coefficient of the resonant frequency ( $\tau_f \sim 0.5$  ppm/°C) [1]. It can form a disordered-type structure (Zn and Ta cations are arranged in a random way over the  $B$  site) with a cubic phase ( $Pm\bar{3}m$  space group) and a 1:2 ordered-type structure (Zn and Ta cations are arranged in Zn–Ta–Ta sequences) with a hexagonal phase ( $P3m1$  space group) [1, 3]. Generally,  $Q$  factor values are improved with the superlattice ordering enhancement by a long annealing time ( $\sim 100$  h), when small ordered domains nucleate and grow in a disordered matrix [1, 3, 4]. However, not only the ordering of  $B$  site cations in the perovskite structure, but also the ceramic microstructure plays an important role in determining the  $Q$  factor values of BZT resonators. On another hand, sintering at temperatures above 1500 °C or an extended thermal treatment leads to partial ZnO volatilization from the surface of BZT samples, which determines the formation of zinc-deficient phases, such as Ba<sub>8</sub>ZnTa<sub>6</sub>O<sub>24</sub>, Ba<sub>3</sub>Ta<sub>2</sub>O<sub>8</sub> or BaTa<sub>2</sub>O<sub>6</sub> [1, 4, 5].

The ordinary technique for preparing BZT ceramic is the conventional solid-state reaction method. However, this compound has a poor sinterability [1, 5-7] and many

investigations have been carried out in order to reduce the sintering parameters without affecting the microwave dielectric properties of BZT resonators. Several authors reported improvements in sinterability by using sintering aids or dopants or by adding glasses [1, 8-10]. Soft chemistry techniques have been also used, but, in most cases, the microwave dielectric properties values were diminished [11, 12].

In this paper, we report on the synthesis and characterization of BZT ceramics doped with Nb<sup>5+</sup>, Ce<sup>4+</sup> or Yb<sup>3+</sup>. The dopants were added in order to improve the densification, granular growth and  $Q \times f$  product values of BZT resonators. The pellets were sintered at 1400, 1500 or 1600°C, for 2 h. The sinterability, phase composition, crystalline structure, microstructure and microwave dielectric properties were investigated and correlations were established.

## 2. Experimental procedure

BZT ceramics doped with Nb<sup>5+</sup>, Ce<sup>4+</sup> or Yb<sup>3+</sup> were prepared from analytical grade reagents by the conventional solid-state reaction method. Starting materials (BaCO<sub>3</sub>, ZnO and Ta<sub>2</sub>O<sub>5</sub>) were weighted according to the compound stoichiometry, homogenised, ball milled and dried. The dry precursor mixture was uniaxial pressed into discs and calcined at 1310 °C, for 2 h, in air, then the discs were ball milled. The resulting powder and the oxide dopants (Nb<sub>2</sub>O<sub>5</sub>, CeO<sub>2</sub> and Yb<sub>2</sub>O<sub>3</sub>) were weighted according to the desired compositions (0.125, 0.25, 0.5 or 1 mol% dopant), homogenised, ball milled and dried. The ground powders were granulated with polyvinyl alcohol (3 mol%) and uniaxial pressed at 150 MPa into pellets ( $\sim 7$  mm diameter and  $\sim 9$  mm height). The pellets were sintered at 1400, 1500 or 1600 °C, for 2 h, in air.

The bulk relative density ( $\rho_r$ ) of BZT sintered samples was measured by Archimede's method, in alcohol. The phase composition and crystal structure of BZT pellets were examined by X-ray diffraction (XRD), using a Shimadzu XRD 6000 diffractometer with Ni filtered Cu-K $\alpha$  radiation,  $2\theta$  ranging between 10 and 80 °. The microstructure of BZT ceramics was investigated with a Hitachi S-2600N scanning electron microscope (SEM). The microwave dielectric properties of BZT resonators, at room temperature, were measured with a Computer Aided Measurement System containing an HP 8757 C Scalar Network Analyser and an HP 8350 B Sweep Oscillator. The dielectric constant ( $\epsilon_r$ ) was obtained with the help of Hakki - Coleman method, using the TE011 mode, while the quality factor ( $Q$ ) was calculated from the TE01 $\delta$  mode by the cavity method.

### 3. Results and discussion

Differential scanning calorimetry analysis of BZT precursor mixture (not presented here) reveals that the formation of BZT compound starts at about 835 °C, fact that has been confirmed by the XRD investigation, and takes place in successive stages of complex solid-state reactions between 835 and 1315 °C, a temperature range in which a structural evolution and a phase composition modification also occur.

It is well known that sintering at temperatures above 1500 °C or a prolonged thermal treatment leads to partial ZnO volatilization at the surface of BZT samples; the weight loss increases with sintering temperature increasing, slowly up to 1500 °C and rapidly above 1500 °C. ZnO depletion determines the formation of zinc-deficient secondary phases, such as Ba<sub>8</sub>ZnTa<sub>6</sub>O<sub>24</sub>, Ba<sub>3</sub>Ta<sub>2</sub>O<sub>8</sub> or BaTa<sub>2</sub>O<sub>6</sub>, which degrade the quality factor of BZT dielectric ceramic [1, 4, 5]. Therefore, ZnO loss during processing (calcination, sintering, annealing) plays an important role in controlling the properties and also the crystal structure of BZT material. Galasso [3] described the evolution of ordered and disordered phases in terms of the nucleation and growth of small ordered domains with increasing annealing time and temperature. Bieringer et al. [13] proposed a mechanism in which a fully ordered BZT phase grows at the expense of a slightly Zn-deficient and partially ordered phase. Moreover, the formation of Zn vacancies from ZnO loss was reported [13] to enhance the cation diffusion and domain growth.

The XRD patterns of BZT ceramics doped with 0.5 or 1 mol% Nb<sub>2</sub>O<sub>5</sub> and sintered at different temperatures are presented in figure 1. XRD investigation was performed on the surface of the samples, without any previous polish, in order to study the influence of the dopants on the secondary phases formation. The sintering treatment parameters influence the formation and stability of BZT compound. XRD analysis indicates a cubic structure for BZT ceramics sintered at 1400 °C; in the case of 1 mol% doping (Fig. 1b), a small amount of zinc-deficient secondary phase is present at BZT sample surface, as a result of partial ZnO volatilization. The drawback effect of the sintering temperature increase from 1400 to 1600 °C consists in the amplification of ZnO loss, which breaks

down the stoichiometry of BZT compound. Above 1400 °C, ZnO depletion accentuates, the amount of BZT decreases rapidly at the samples surface, while the quantity of Ba<sub>8</sub>ZnTa<sub>6</sub>O<sub>24</sub> and BaTa<sub>2</sub>O<sub>6</sub> secondary phases grow up. The first one is Zn-poor (Ba<sub>8</sub>ZnTa<sub>6</sub>O<sub>24</sub>), while the second one is Zn-free (BaTa<sub>2</sub>O<sub>6</sub>) compared to BZT nominal composition. It is interesting to observe that for 1500 °C sintering temperature, the amount of secondary phase is lower in the case of BZT ceramic doped with 1 mol% Nb<sub>2</sub>O<sub>5</sub> than in the case of the one doped with 0.5 mol% Nb<sub>2</sub>O<sub>5</sub>; this behaviour can be attributed to the reduced porosity, as well as quick and pronounced grain growth, obtained for an optimum dopant concentration and sintering temperature. The optimum concentration promotes large grains, with a small number of structural defects, this dense and stable microstructure hindering ZnO volatilization.

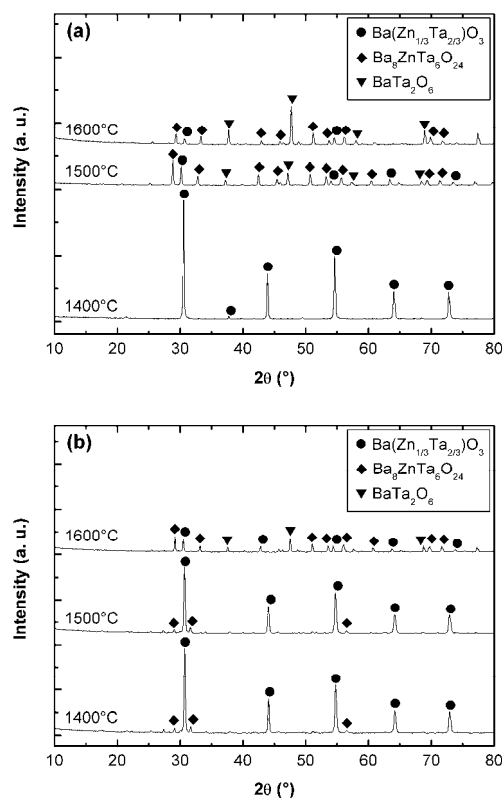


Fig. 1. XRD patterns of BZT ceramics doped with: (a) 0.5 mol% and (b) 1 mol% Nb<sub>2</sub>O<sub>5</sub>, for all sintering temperatures.

Fig. 2 shows the XRD patterns of BZT ceramics doped with CeO<sub>2</sub> (Fig. 2a) or Yb<sub>2</sub>O<sub>3</sub> (Fig. 2b), sintered at 1600 °C. It is obvious that these two dopants have a small ability for the preservation of BZT compound at high temperatures; the two secondary phases mentioned earlier appear for all dopants concentrations. The presence of Ce<sup>4+</sup> leads to a multiphase system even for 0.125 mol% doping; the same observation occurs in the case of Yb<sup>3+</sup> as dopant. BZT represents the major phase only in the case of 0.125 or 0.25 mol% CeO<sub>2</sub> doping, while for 0.5 or 1 mol% Yb<sub>2</sub>O<sub>3</sub> doping, the Zn-free secondary phase (BaTa<sub>2</sub>O<sub>6</sub>)

becomes the dominant phase, associated with the other Zn-poor compound.

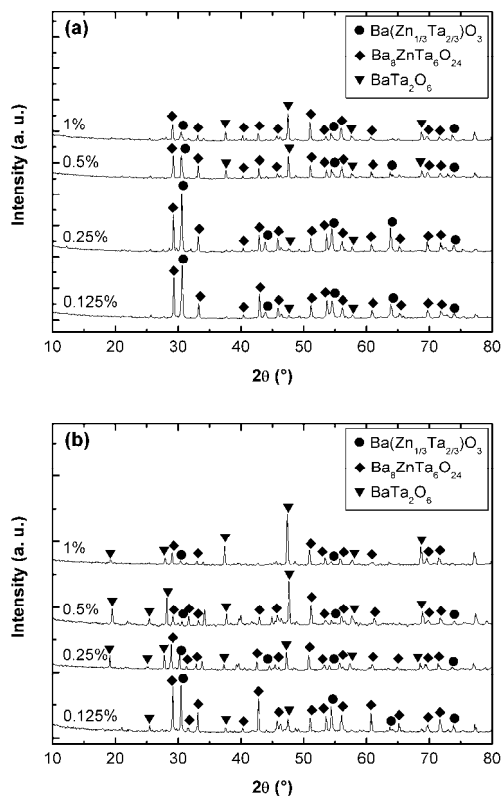


Fig. 2. XRD patterns of BZT ceramics doped with: (a)  $\text{CeO}_2$  and (b)  $\text{Yb}_2\text{O}_3$ , sintered at  $1600\text{ }^\circ\text{C}$ , for all dopant molar concentrations.

It is well known that during sintering, BZT phase crystallizes in a disordered cubic perovskite structure, which on annealing becomes a 1:2 ordered hexagonal structure, with Zn–Ta–Ta repeat sequence along (111) direction of the parent cubic cell. For getting this ordered structure, BZT is normally annealed at temperatures in the range  $1300 - 1400\text{ }^\circ\text{C}$ , for various lengths of time, up to 100 h. The ordered nanodomains appear in small quantities at temperatures below  $1400\text{ }^\circ\text{C}$  even during the sintering process [1, 3], but it is hard to identify the corresponding peaks on our XRD patterns, first because at  $1400\text{ }^\circ\text{C}$ , the quantity of 1:2 ordered BZT phase is smaller than the method detection limit and second because at  $1500$  and  $1600\text{ }^\circ\text{C}$ , the surface presents a high amount of secondary phases and the intensities of BZT peaks decrease very much.

The microstructure of some doped BZT ceramics sintered at different temperatures is presented in Figs. 3 - 6. For all compositions, the increase of the sintering temperature and dopants concentration promotes the granular growth due to the enhancement of the diffusion processes.

In the case of  $\text{Nb}^{5+}$ , all BZT samples sintered at  $1400\text{ }^\circ\text{C}$  present a relative high intergrain porosity and a relative small number of intergrain bridges (Fig. 3a and Fig. 4a); the uniaxial pressing process and the deficient sintering temperature can be two of the reasons for these porous structures. The increase of the sintering

temperature from  $1400$  to  $1500\text{ }^\circ\text{C}$  determines the intensification of the bridge diffusion process, so that the porosity decreases, but the grain average size remains the same or increases very little, around  $0.5\text{ }\mu\text{m}$  for  $0.5\text{ mol}\%$  (Fig. 3b) and around  $0.8\text{ }\mu\text{m}$  for  $1\text{ mol}\%$   $\text{Nb}_2\text{O}_5$  doping (Fig. 4b). For  $1600\text{ }^\circ\text{C}$  sintering temperature,  $\text{Nb}^{3+}$  doped BZT ceramics are well densified and reveal spherical or polyhedral grains with rounded edges and corners, with dimensions in the range  $0.5 - 2.5\text{ }\mu\text{m}$  for  $0.5\text{ mol}\%$   $\text{Nb}_2\text{O}_5$  doping (Fig. 3c). The larger grains were obtained in the case of  $1\text{ mol}\%$   $\text{Nb}_2\text{O}_5$  doping and  $1600\text{ }^\circ\text{C}$  sintering temperature, with dimensions up to  $7\text{ }\mu\text{m}$  (Fig. 4c); the SEM image of this sample reveals the fact that during the sintering process, a liquid phase is formed; this phase fills in the spaces between grains and after cooling it crystallizes. If we corroborate the information given by the XRD and SEM analyses, we can say that the compound that melts and crystallizes is  $\text{BaTa}_2\text{O}_6$  secondary phase.

The microstructure of BZT ceramic that presents the best microwave dielectric properties (see Fig. 8a) is shown in figure 3c. Although the grains of this sample are not the biggest, the dielectric loss of the resonator made from this material is the lowest.

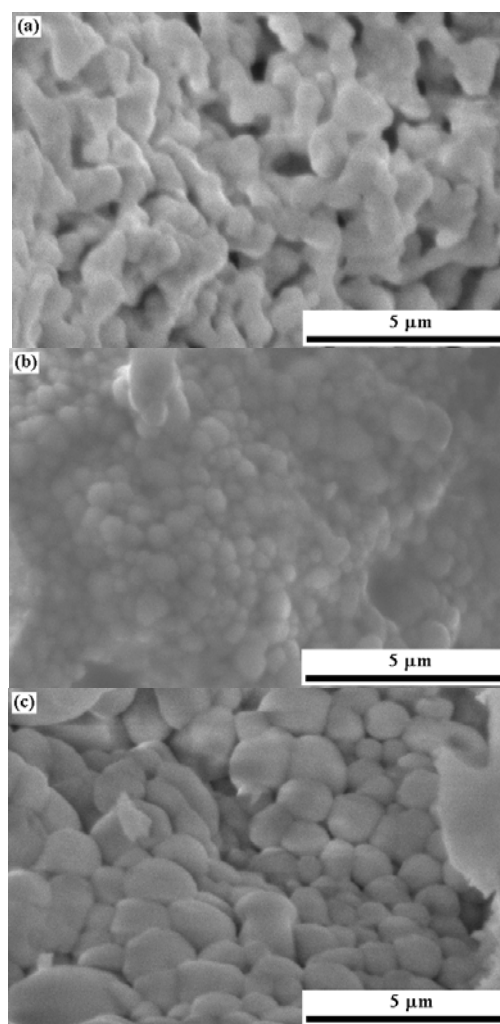


Fig. 3. SEM images of BZT ceramics doped with  $0.5\text{ mol}\%$   $\text{Nb}_2\text{O}_5$ , sintered at: (a)  $1400\text{ }^\circ\text{C}$ , (b)  $1500\text{ }^\circ\text{C}$  and (c)  $1600\text{ }^\circ\text{C}$ .

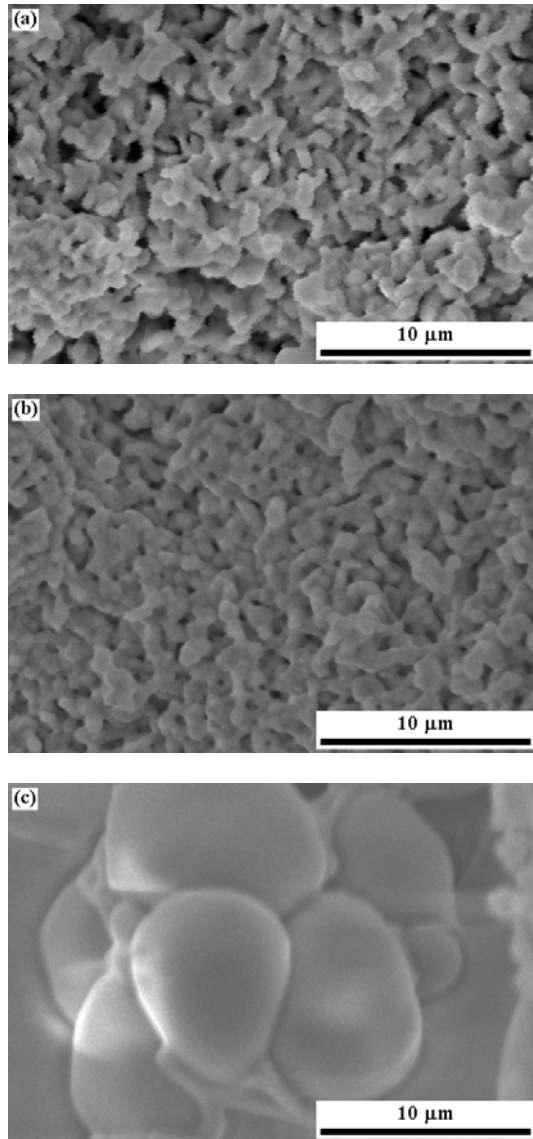


Fig. 4. SEM images of BZT ceramics doped with 1 mol% Nb<sub>2</sub>O<sub>5</sub>, sintered at: (a) 1400 °C, (b) 1500 °C and (c) 1600 °C.

The use of Ce<sup>4+</sup> as dopant induces complex modifications regarding the morphology of BZT ceramics (Fig. 5). The secondary phases indicated by the XRD investigation can be also observed in all SEM images, resulting in a heterogeneous microstructure. In the case of 0.125 mol% CeO<sub>2</sub> doping, the sample surface presents bunches of BZT grains with an average size of about 1 μm, but also secondary phases columns, with lengths that can exceed 10 μm. All the other three compositions have similar morphologies, composed of large grains, sometimes much bigger than 10 μm, due to the intense liquid diffusion processes that take place during the sintering treatment, followed by crystallization during the cooling stage.

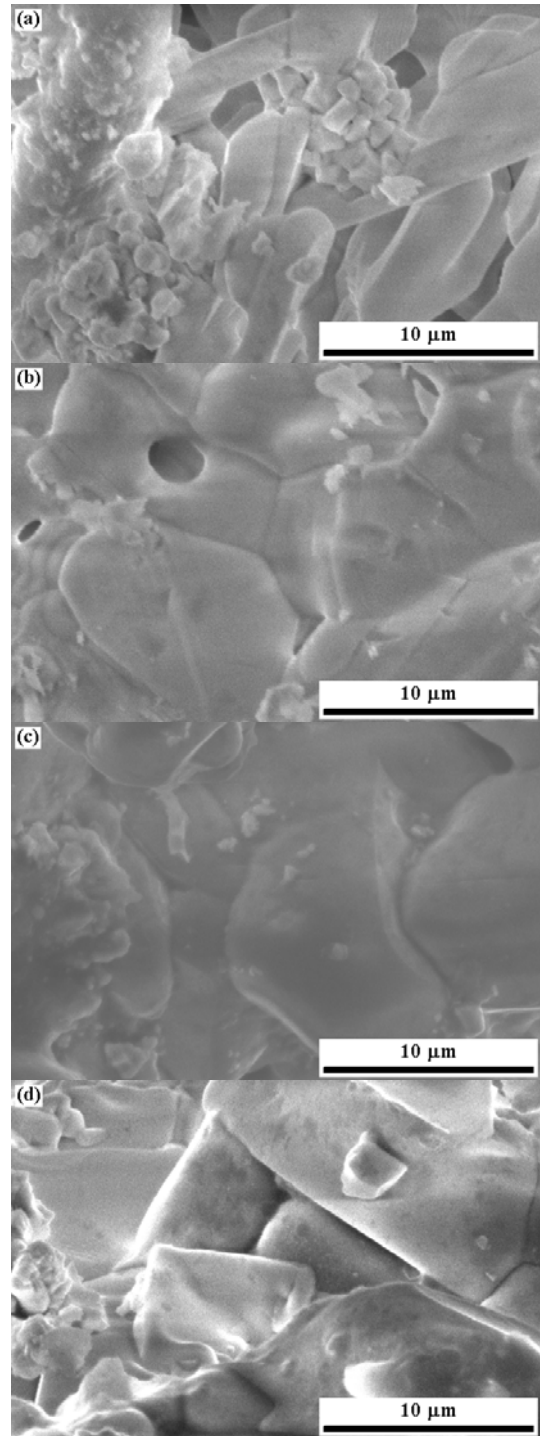


Fig. 5. SEM images of BZT ceramics doped with: (a) 0.125 mol%, (b) 0.25 mol%, (c) 0.5 mol% and (d) 1 mol% CeO<sub>2</sub>, sintered at 1600 °C.

In the case of using Yb<sup>3+</sup> as dopant, the increase of the amount of secondary phases with dopant concentration increasing can be very well observed. For 0.125 mol% Yb<sub>2</sub>O<sub>3</sub> doping (Fig. 6a), the SEM image presents a cluster of grains with bimodal size distribution (with maxima at approximately 2.5 and 5 μm) surrounded by a small quantity of secondary phases; if the dopant concentration is increased at 0.25 mol% (Fig. 6b), the little grains are swallowed by the liquid phases formed during the thermal

treatment, obtaining a microstructure with near-zero intergrain porosity. When the dopant concentration reaches 0.5 mol% (Fig. 6c), the morphology of BZT ceramic consists in isolated large grains enclosed in an almost continuous secondary phases matrix, while for 1 mol% doping, the pellet surface presents domains larger than 6  $\mu\text{m}$ , formed by the crystallization of the liquid phases.

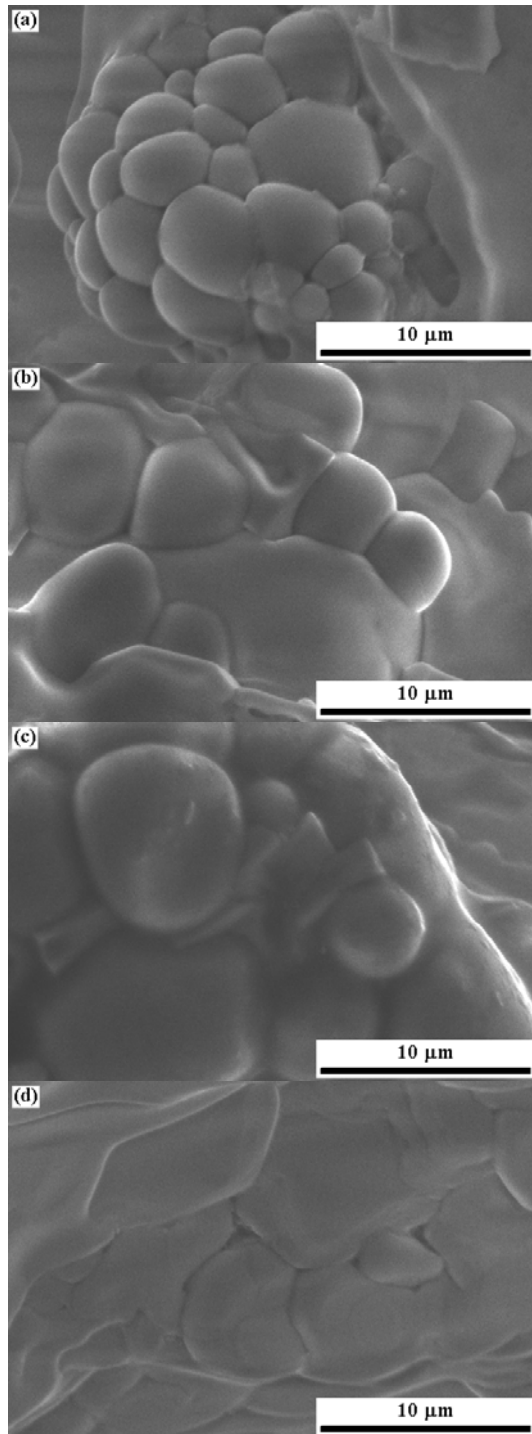


Fig. 6. SEM images of BZT ceramics doped with: (a) 0.125 mol%, (b) 0.25 mol%, (c) 0.5 mol% and (d) 1 mol%  $\text{Yb}_2\text{O}_3$ , sintered at 1600 °C.

The bulk relative density of doped BZT ceramics was determined after the sintering process and the resulted values are shown in figure 7, as a function of the dopants concentration, for all sintering temperatures. Moreover, Fig. 7 presents the values of the dielectric constant because it is well known that the bulk relative density and dielectric constant are strongly correlated. It can be seen that the dependence of these two parameters on the dopant type and quantity and on the sintering temperature presents the same trend. From ceramic and dielectric point of view,  $\text{Nb}^{5+}$  is the most efficient dopant; for 1500 °C sintering temperature, three of the bulk relative density values are above 95 % and the corresponding dielectric constant values above 28. In the case of  $\text{Nb}_2\text{O}_5$ , the increase of the sintering temperature from 1500 to 1600 °C has a negative influence, as it can be seen in figure 7a, as a consequence of partial  $\text{ZnO}$  volatilization at the samples surface.

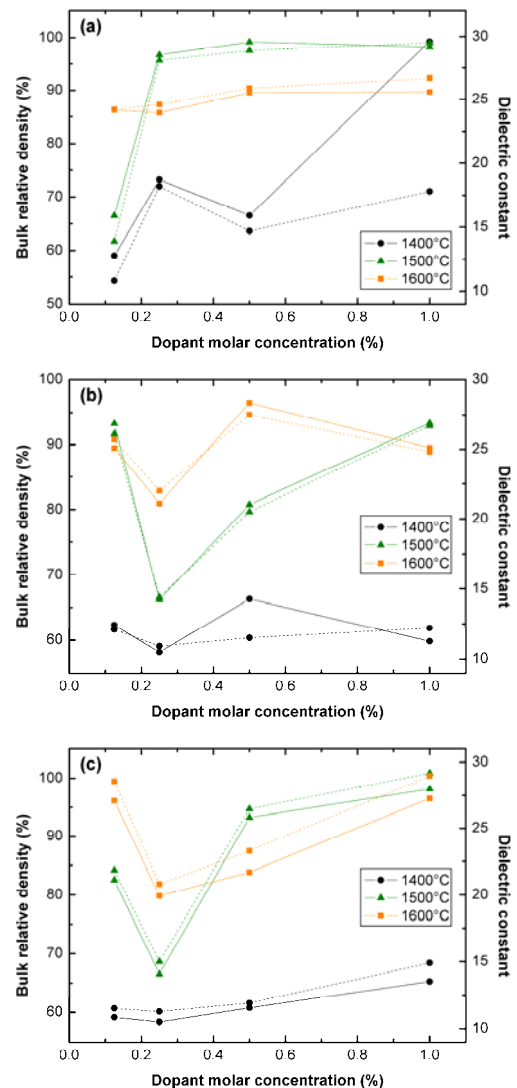


Fig. 7. Bulk relative density (solid line) and dielectric constant (dashed line) of BZT ceramics doped with: (a)  $\text{Nb}_2\text{O}_5$ , (b)  $\text{CeO}_2$  and (c)  $\text{Yb}_2\text{O}_3$  versus dopant molar concentration, for all sintering temperatures.

In the case of CeO<sub>2</sub> and Yb<sub>2</sub>O<sub>3</sub>, the change of the dopant concentration and sintering temperature determines a random behaviour (Fig. 7b and Fig. 7c). For example, the values obtained for the bulk relative density and dielectric constant for 0.25 mol% doping are the lowest for all sintering temperatures, this meaning that a concentration of 0.25 mol% has a negative influence on the densification, which leads to poor dielectric constant values.

As a conclusion, BZT samples with a good compactness and a high dielectric constant were obtained by using more than 0.25 mol% Nb<sub>2</sub>O<sub>5</sub> and sintering at 1500 °C, 0.5 mol% CeO<sub>2</sub> / 1600 °C, 125 mol% Yb<sub>2</sub>O<sub>3</sub> / 1600 °C and 1 mol% Yb<sub>2</sub>O<sub>3</sub> / 1500 °C or 1600 °C.

Microwave measurements were performed in the 5 - 12 GHz frequency range. Figure 8 presents the variation of the  $Q \times f$  product (the product between the quality factor and the resonant frequency) of BZT resonators versus sintering temperature, for all dopants concentrations. Generally, the increase of the sintering temperature has a positive influence on the dielectric loss, this being attributed to the fact that a high sintering temperature promotes the granular growth and reduces the number of grain boundaries, as well as the concentration of other structural defects that are involved in the dielectric loss mechanism. Only the sample doped with 0.25 mol% Nb<sub>2</sub>O<sub>5</sub> presents a small decrease of the  $Q \times f$  product when increasing the sintering temperature from 1500 to 1600 °C, probably due to the intensification of ZnO depletion, which leads to a higher amount of secondary phases. In the case of Nb<sup>5+</sup>, the best  $Q \times f$  product value, ~ 159 THz, was registered for 0.5 mol% doped BZT ceramic, sintered at 1600 °C.

BZT samples doped with Ce<sup>4+</sup> exhibit a very irregular behaviour and there can not be made correlations between the  $Q \times f$  product values and the compositional parameters. 0.125 mol% doping seems to be the optimal dopant concentration in this case, for which a value of ~ 78 THz was achieved when sintering at 1600 °C; all the other values remain below 41 THz.

In the case of Yb<sup>3+</sup>, the dopant concentration has not a substantial influence on the dielectric loss, for each sintering temperature, the  $Q \times f$  product values being very close; the increase of the sintering temperature from 1400 to 1500 °C determines an increase of 2.2 - 3.4 times, while the increase of the sintering temperature from 1500 to 1600 °C leads to an increase of 2 - 2.7 times of the same parameter discussed earlier. The highest value of the  $Q \times f$  product is ~ 49 THz, attained in the case of 1 mol% doping and 1600 °C sintering temperature.

The quality factor of complex perovskite microwave materials is very sensitive to a number of different processing and structural variables. It can vary from sample to sample even when they have the same nominal composition due to small differences in the intrinsic crystal structure, microstructure, density and impurity concentration, cationic order and stoichiometry [1]. Moreover, it is well known that the formation of secondary phases leads to a decrease of the quality factor [1, 4, 5].

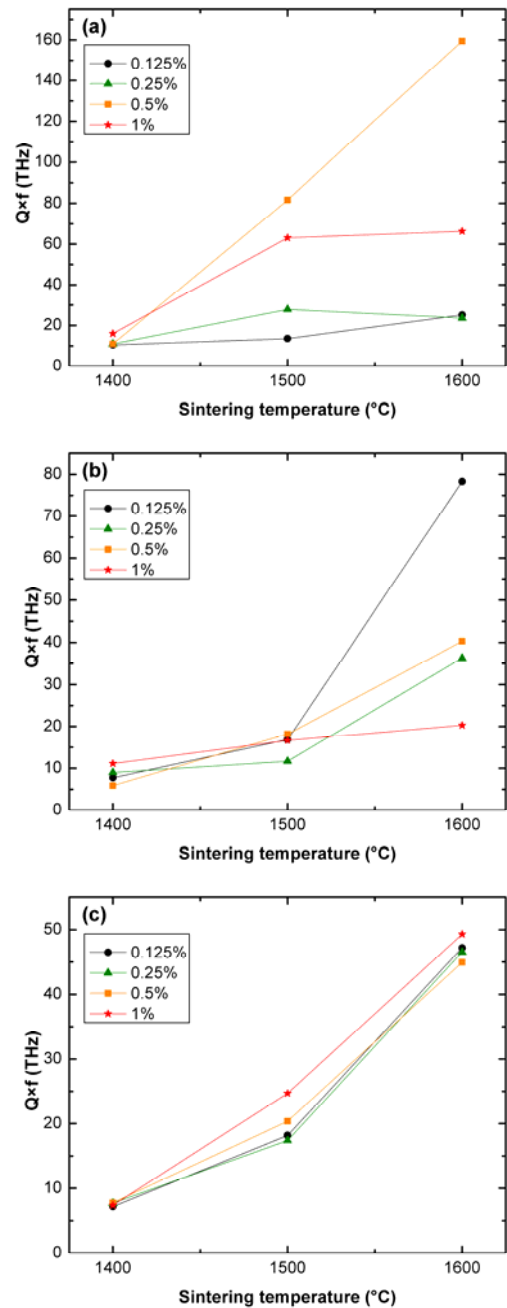


Fig. 8.  $Q \times f$  product of BZT ceramics doped with: (a) Nb<sub>2</sub>O<sub>5</sub>, (b) CeO<sub>2</sub> and (c) Yb<sub>2</sub>O<sub>3</sub> versus sintering temperature, for all dopant molar concentrations.

The highest  $Q \times f$  product value (~ 210 THz) ever reported for BZT material was attained in the case of 0.95Ba(Zn<sub>1/3</sub>Ta<sub>2/3</sub>)O<sub>3</sub>-0.05(Sr<sub>0.25</sub>Ba<sub>0.75</sub>)(Ga<sub>1/2</sub>Tad<sub>1/2</sub>)O<sub>3</sub> ceramic sintered at 1550 °C / 2 h and annealed at 1450 °C / 24 h [14], while the second highest  $Q \times f$  product value (~ 200 THz) was achieved with the addition of 1 mol% BaWO<sub>4</sub>, for 1580 °C / 3 h sintered sample [15].

In our study, the highest value for the  $Q \times f$  product (~ 159 THz) was obtained in the case of BZT resonator doped with 0.5 mol% Nb<sub>2</sub>O<sub>5</sub> and sintered at 1600 °C / 2 h. It is obvious that the value is very good if we take into account the fact that this result was attained without any annealing treatment.

Ioachim et al. [8] investigated the effect of different dopants (Nb, Zr, Eu, Al+Y) on the microwave properties of BZT ceramics. The  $\epsilon_r$  values for the un-annealed doped BZT samples are in the range 26.5 - 28.5. The highest  $Q \times f$  product values, up to 35 THz, were obtained for those samples doped with 1 mol% Nb, 1 mol% Eu or 0.5 mol% Al + 0.5 mol% Y, all sintered at 1550 °C / 2 h. The annealing treatment at 1410 °C / 30 h leads to  $Q \times f$  product values between 80 and 90 THz for Nb, Eu or Al+Y doped BZT ceramics sintered at temperatures higher than 1500 °C / 2 h and to ~ 98 THz for Zr doped BZT ceramic sintered at 1400 °C / 3 h. In this paper, the  $\epsilon_r$  values start from 10.5, but they reach 29.5 for the best pellet. Moreover, without any annealing treatment, the highest  $Q \times f$  product values for each dopant are: ~ 159 THz for Nb<sup>5+</sup>, ~ 78 THz for Ce<sup>4+</sup> and ~ 49 THz for Yb<sup>3+</sup>.

Varma et al. [9, 10] made a detailed investigation on the effect of dopants addition in BZT. They added several dopants of varying valence, ionic size and concentration and studied the variations in densification and microwave dielectric properties. It was found that the quality factor increases when the ionic radius of the dopant is close to that of the B site ions (Zn - 0.74 Å and Ta - 0.64 Å). The highest  $Q \times f$  product values were obtained for doping with Zr, Cr or Ce. The authors concluded that by introducing long range cation order by prolonged annealing at temperatures above 1350 °C and by adding a small amount of suitable dopants, the  $Q \times f$  product of BZT resonators can be increased up to 200 THz. Taking this explanation into consideration, it is obvious why Nb<sup>5+</sup> has a positive effect on the quality factor of our BZT resonators: the ionic radius of this ion coordinated with six oxygen ions is 0.640 Å, that is exactly the same value for Ta<sup>5+</sup>. The other two ions, Ce<sup>4+</sup> and Yb<sup>3+</sup>, present ionic radii of 0.870 Å and 0.868 Å, respectively. It was also reported that the quality factor is very much improved by some dopants although the order parameter is decreased. Since Nb<sup>5+</sup> improves the quality factor, it implies that it substitutes for Zn or Ta in BZT structure, while Ce<sup>4+</sup> and Yb<sup>3+</sup> do not penetrate into the network, but they favour the secondary phases formation.

#### 4. Conclusions

Doped Ba(Zn<sub>1/3</sub>Ta<sub>2/3</sub>)O<sub>3</sub> (BZT) ceramics were prepared by the conventional solid-state reaction method, being sintered at 1400, 1500 or 1600 °C / 2 h. Nb<sub>2</sub>O<sub>5</sub>, CeO<sub>2</sub> or Yb<sub>2</sub>O<sub>3</sub> were used as dopants.

XRD investigation reveals the formation of BZT compound, but also the appearance of relative high amounts of secondary phases at the samples surface, as a result of partial ZnO volatilization, especially at high temperatures. The secondary phases are Zn-poor (Ba<sub>8</sub>ZnTa<sub>6</sub>O<sub>24</sub>) or Zn-free (BaTa<sub>2</sub>O<sub>6</sub>) compared to BZT nominal composition. The samples sintered at 1400 °C present a disordered cubic structure, while in the case of those sintered at 1500 or 1600 °C we can suppose that they contain the 1:2 ordered phase in some proportion, this being responsible for the high  $Q \times f$  product values.

Generally, bulk relative density, grain size and dielectric constant increase with dopants concentration and sintering temperature increasing. The efficiency of the

dopants used in this study decreases in the range Nb<sub>2</sub>O<sub>5</sub> > CeO<sub>2</sub> > Yb<sub>2</sub>O<sub>3</sub>. Dopant type has a strong influence on the secondary phases formation, but also on the microstructure. BZT resonator doped with 0.5 mol% Nb<sub>2</sub>O<sub>5</sub> and sintered at 1600 °C exhibits the highest  $Q \times f$  product value, ~ 159 THz, with a dielectric constant value of ~ 25.9.

#### Acknowledgements

The work has been partially funded by the Sectoral Operational Programme Human Resources Development 2007 - 2013 of the Romanian Ministry of Labour, Family and Social Protection through the Financial Agreement POSDRU/88/1.5/S/61178.

#### References

- [1] M.T. Sebastian, Dielectric Materials for Wireless Communication, Elsevier Ltd., 2008
- [2] K. M. Luk, K.W. Leung, Dielectric Resonator Antennas, Research Studies Press Ltd., Baldock, Hertfordshire, England, 2003
- [3] F.S. Galasso, Structure and Properties of Perovskite Compounds, Pergamon Press, Headington Hill, Oxford, England, 1969
- [4] P.K. Davies, A. Borisevich, M. Thirumal, J. Eur. Ceram. Soc. **23**, 2461 (2003).
- [5] A. Ioachim, M.I. Toacsan, M.G. Banciu, L. Nedelcu, C.A. Dutu, M. Feder, C. Plapcianu, F. Lifei, P. Nita, J. Eur. Ceram. Soc. **27**, 1117 (2007).
- [6] L. Nedelcu, M.I. Toacsan, M.G. Banciu, A. Ioachim, J. All. Comp. **509**, 477 (2011).
- [7] A. Ioachim, L. Nedelcu, E. Andronescu, S.I. Jinga, M.I. Toacsan, M.G. Banciu, A. Lorinczi, M. Popescu, J. Optoelectron. Adv. Mater **10**(1) 209 (2008).
- [8] A. Ioachim, M.I. Toacsan, L. Nedelcu, M.G. Banciu, C.A. Dutu, E. Andronescu, S.I. Jinga, P. Nita, H.V. Alexandru, J. Optoelectron. Adv. Mater. **9**(6) 1833 (2007).
- [9] M.R. Varma, R. Reghunathan, M.T. Sebastian, Jpn. J. Appl. Phys. **44**, 298 (2005).
- [10] M.R. Varma, N.D. Kataria, J Mater Sci: Mater Electron **18**, 441 (2007).
- [11] M.R. Varma, P. Nisha, P.C.R. Varma, J. All. Comp. **457**, 422 (2008).
- [12] C. Jinga, D. Berger, C. Matei, S. Jinga, E. Andronescu, J. All. Comp. **497**, 239 (2010).
- [13] M. Bieringer, S.M. Moussa, L.D. Noailles, A. Burrows, C.J. Kiely, M.J. Rossinsky, R.M. Ibberson, Chem. Mater. **15**, 586 (2003).
- [14] K. Kageyama, J. Am. Ceram. Soc. **75**(7) 1767 (1992).
- [15] J.S. Kim, J.W. Kim, C.I. Cheon, Y.S. Kim, S. Nahm, J.D. Byun, J. Eur. Ceram. Soc. **21**, 2599 (2001).

\*Corresponding author: sorinionjinga@yahoo.com